

# Accelerated functional brain aging in major depressive disorder: evidence from a large scale fMRI analysis of Chinese participants

Yunsong Luo,<sup>1</sup> Wenyu Chen,<sup>1</sup> Jiang Qiu,<sup>2,3,4</sup> and Tao Jia<sup>1,\*</sup>

<sup>1</sup>*College of Computer and Information Science,  
Southwest University, Chongqing, 400715, P. R. China*

<sup>2</sup>*Key Laboratory of Cognition and Personality(SWU),  
Ministry of Education, Chongqing, 400715, P. R. China*

<sup>3</sup>*School of Psychology, Southwest University (SWU), Chongqing,400715, P. R. China*

<sup>4</sup>*Southwest University Branch, Collaborative Innovation Center of Assessment Toward  
Basic Education Quality at Beijing Normal University,Chongqing, 400715, P. R. China*

(Dated: May 11, 2022)

## Abstract

Major depressive disorder (MDD) is one of the most common mental health conditions that has been intensively investigated for its association with brain atrophy and mortality. Recent studies reveal that the deviation between the predicted and the chronological age can be a marker of accelerated brain aging to characterize MDD. However, current conclusions are usually drawn based on structural MRI information collected from Caucasian participants. The universality of this biomarker needs to be further validated by subjects with different ethnic/racial backgrounds and by different types of data. Here we make use of the REST-meta-MDD, a large scale resting-state fMRI dataset collected from multiple cohort participants in China. We develop a stacking machine learning model based on 1101 healthy controls, which estimates a subject's chronological age from fMRI with promising accuracy. The trained model is then applied to 1276 MDD patients from 24 sites. We observe that MDD patients exhibit a +4.43 years ( $p < 0.0001$ , Cohen's  $d = 0.35$ , 95% CI : 1.86 – 3.91) higher brain-predicted age difference (brain-PAD) compared to controls. In the MDD subgroup, we observe a statistically significant +2.09 years ( $p < 0.05$ , Cohen's  $d = 0.134483$ ) brain-PAD in antidepressant users compared to medication-free patients. The statistical relationship observed is further checked by three different machine learning algorithms. The positive brain-PAD observed in participants in China confirms the presence of accelerated brain aging in MDD patients. The utilization of functional brain connectivity for age estimation verifies existing findings from a new dimension.

---

\* t.jia@swu.edu.cn

## 1. INTRODUCTION

Global population aging is expected to be one of the prominent social changes of the 21st century [1]. The resulting burden of age-related functional decline and disease would challenge all sectors of society, especially healthcare [2]. Therefore, understanding the biological link between aging and disease risk becomes increasingly important to provide effective care and treatment [3]. Aging can be regarded as a dynamic process in which an individual gradually loses her function as cumulative age-related damage accumulates. The brain structure and function are also significantly changed during this process [4]. As the central nervous system may age dissimilarly to the rest of the body [5], brain-specific aging markers may be of particular importance in assessing the risk of cognitive decline and propensity to neurodegenerative diseases [6, 7].

Accelerated aging of the brain refers to the phenomenon that an individual’s brain appears older compared with the expected chronological age. Brain predicted age difference (brain-PAD), calculated as the difference between the estimated brain age from neuroimaging and the chronological age, is predisposed to be associated with the risk of cognitive aging or age-related brain disorders. This neuroimaging-based biomarker is observed in several neurological disorders [8, 9], including schizophrenia [10–12], Alzheimer’s disease [13–15], epilepsy [16], multiple sclerosis [17], and traumatic brain injury [18]. Furthermore, an association between brain-PAD and mortality [19] has also been reported.

Recent research set out to explore the relationship between accelerated brain aging and major depressive disorder (MDD), a widespread, debilitating, and disabling psychiatric disorder [20] associated with cellular senescence [21, 22] and cognitive decline [23]. Despite the positive association reported [11, 24–28], current studies still present several limitations. First, the size of samples can have a great influence on the stability of the relationship discovered. While subjects with diverse sizes are investigated [8, 29], only one study analyzes data from more than 1,000 individuals [30], to the best of our knowledge. Moreover, most of the current studies are based on Caucasian subjects. In the meanwhile, the brain age is usually estimated from the structural MRI, with the grey or white matter volume and cortical thickness as the key feature. The generalizability of the association needs to be further verified in subjects from different ethnic and cultural backgrounds and tested by other types of neuroimaging data. Finally, previous studies often rely on only one machine learning

algorithm to estimate brain age. Since different algorithms yield different estimations, it is reasonable to suspect that the conclusion drawn is algorithm sensitive. The statistically significant association originally reported may vanish when a new algorithm is applied.

To cope with these limitations, we make use of the resting-state functional magnetic resonance imaging (rsfMRI) data [31] collected by the REST-meta-MDD [32, 33], which is a coordinated multisite project from China containing over 1000 MDD patients and normal controls. We utilize three different machine learning algorithms to estimate brain age from resting-state functional connectivity [34–36]. We further propose a stacking model to combine results from the three algorithms to reach a more optimal age estimation. We conduct separate analyses on results obtained from each algorithm to check the robustness of the conclusion drawn. We confirm the existence of the positive association between accelerated brain aging and MDD based on subjects in China. The brain-PAD is significantly higher in MDD patients compared to controls and the conclusion is not affected by the machine learning algorithm applied. We separately analyze MDD patients with different depression severity, illness duration, episode status, and medication status to investigate the association between brain-PAD with demographic (age, sex) and clinical characteristics. We find a significant correlation between brain-PAD and illness duration in MDD patients as well as a higher brain-PAD in antidepressant users than in medication-free patients.

## 2. METHODS

### 2.1. Samples

We conduct this study through rsfMRI indices of MDD patients and matched controls (aged 12-82 years) from the REST-meta-MDD consortium, which consists of 25 research groups from 17 hospitals in China. All MDD patients are hospital diagnosed and conducted at least a T1-weighted structural scan and a rsfMRI scan. All subjects agree to provide diagnosis, age, gender, and education years. The 17-item Hamilton Depression Rating Scale (HDRS) is administered to some patients with other tabular data provided, including episode status (if the patient’s prior and current episodes are diagnosed as MDD according to ICD10 or DSM-IV), medication status (whether antidepressants are used), and illness duration. After quality control, we reach a sample set of 1276 MDD patients and 1101 controls from 24

sites. Additional details regarding inclusion and exclusion criteria, demographic measures, and medication status are provided in Supplementary Table S1 and Table S2. Written informed consent is signed by participants at each local site, and all data are de-identified and anonymized. Besides, approvals from the local institutional review board and ethics committee are granted at all sites.

## **2.2. rsfMRI data preprocessing and functional brain network construction**

The Data Processing Assistant for Resting State fMRI (DPARSF) [37] is used as a standardized preprocessing pipeline. To obtain the functional connectivity, we first extract 116 averaged blood oxygen level-dependent (BOLD) signals based on the Automated Anatomical Labeling (AAL) atlas. Next, we calculate the Pearson correlation coefficients between the BOLD activity time series. Fisher’s r-to-z transform is applied to get the whole-brain functional network from the functional connectivity matrix of each subject. More details of the data preprocessing process are presented in Supplementary Information S2.

## **2.3. Model training and evaluation**

To obtain the input feature for the model, we reshape the upper triangle of the whole-brain correlation matrix into a one-dimensional vector with 6670 elements. To determine the brain aging pattern in healthy individuals, we first train a brain age prediction model on the training set containing 1101 normal controls. Next, we utilize the model to estimate the brain age of 1276 MDD patients on the test set. The brain age prediction is first carried out by three classical supervised learning algorithms: elastic net [38, 39], bayesian ridge [40], and ridge regression [30, 41, 42]. Furthermore, we introduce a stacking model [34] from ensemble learning [43, 44] to combine results from the three algorithms, which gives the best estimation results. The flow is shown in Fig. 1 and Supplementary Fig. S1. The four models all come to consistent conclusions in subsequent experiments. To avoid switching between different methods and make the flow of the paper more concise, we use the results from the stacking method in the main text. Analyses based on the other three algorithms are included in Supplementary Table S3.

We evaluate our model performance in the control and MDD groups separately. We

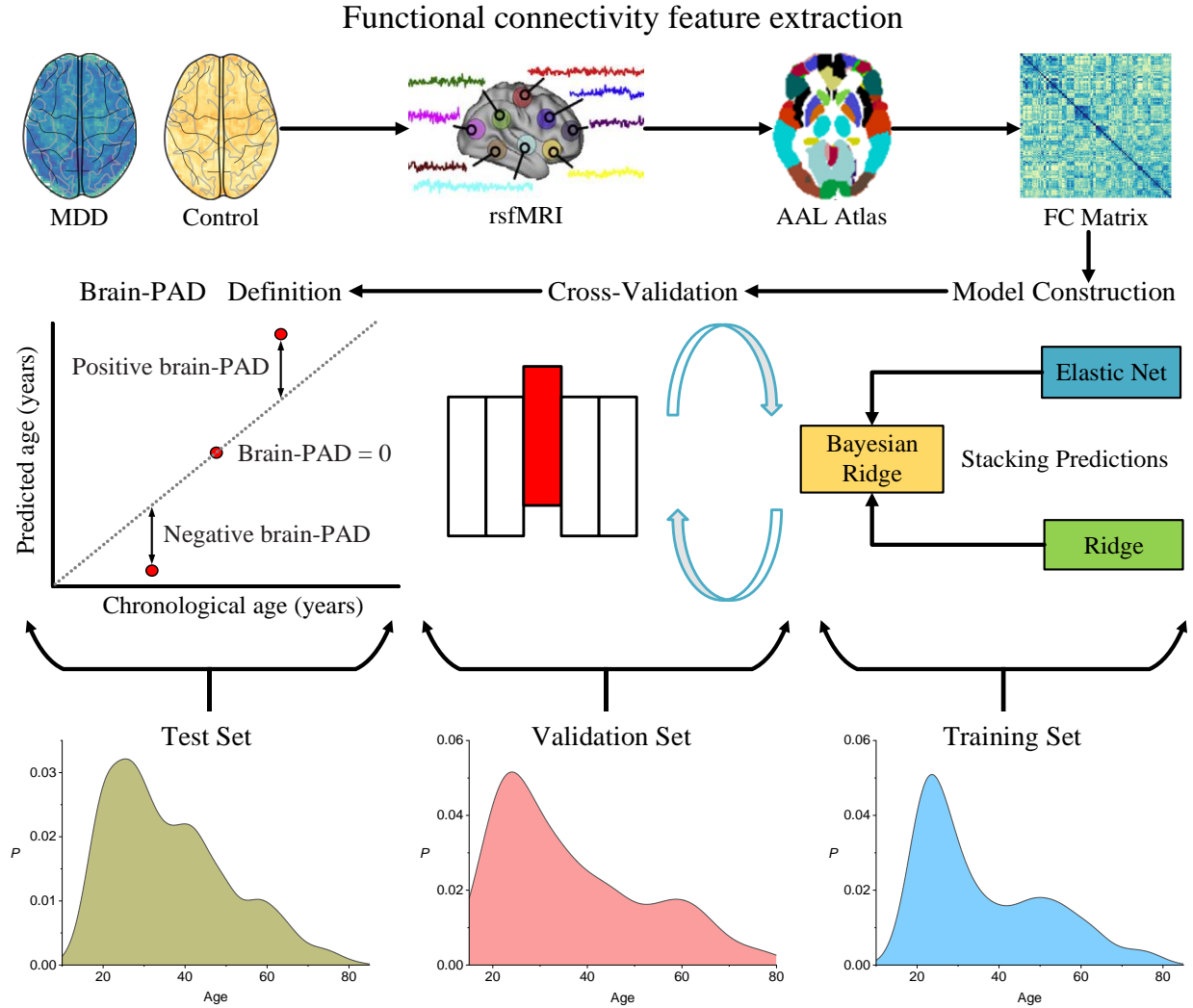


Fig. 1: The flow chart of the analysis. Time series for each subject are extracted from rsfMRI according to the AAL atlas.

The Pearson correlation is used to get the functional connectivity matrix. Next, the upper triangle of the functional connectivity matrix is stretched into a one-dimensional vector to get each subject's feature vector. The feature vectors are concatenated to obtain input data matrices. A brain age prediction model is trained and five-fold cross-validated on the training set. Finally, brain-PAD scores are obtained by applying the model in the hold-out validation set and test set.

first evaluate the model on the entire training set with five-fold cross-validation. Then, the same model in each fold is used to predict the brain age of MDD patients on the entire test set. The performance of the four models is evaluated based on the following three metrics: mean absolute error (MAE), mean squared error (MSE) and mean coefficient of determination ( $R^2$ ). All models are implemented through the Python-based sklearn package with all parameters set as the default value.

## 2.4. Statistical analyses

To determine whether brain aging is accelerated in MDD patients relative to controls, we split the entire controls to get a fixed training set and a validation set using the hold-out method [45]. While modest in size, this hold-out validation set consists of normal controls from all sites with the entire age span, providing an unbiased age representation of Rest-meta-MDD. We obtain a model on the training set and use it to estimate the brain age of the normal controls in the hold-out validation set and all MDD patients in the test set. The chronological age is subtracted from the estimated age to get the brain-PAD as the outcome variable for statistical analysis. The five-fold cross-validation is used to compare the overall performance of different models. The hold-out validation set is used as a normal control group for brain-PAD comparison. Due to factors such as regression dilution and non-Gaussian age distribution [46], we need to perform an age-bias correction. We apply a posthoc correction for the residual age effect on the test set [41, 47–50]. Following Peng et al. [51], we first train a linear regression model on the hold-out validation set to fit the predicted age with the chronological age labels. The slope and intercept of the fitting line are then used to correct the predicted age of the MDD patients in the test set. The systematic bias and the corresponding correction method are illustrated in Supplementary Fig. S2 and Fig. S3. We apply the univariate generalized linear model (GLM) with gender, diagnosis, age, and age<sup>2</sup> as covariates to explore the relationship between brain-PAD and clinical characteristics [27]. Furthermore, the two-sample t-test is used to compare the brain-PAD in different subgroups. Multiple comparisons are corrected by false discovery rates correction. The threshold for statistical significance is set at  $p < 0.05$ .

## 3. RESULTS

### 3.1. Model performance

The models obtained from each fold of the training set are used to estimate the brain age of individuals for the rest of the controls in the validation set as well as the MDD patients in the test set. Table 1 shows the performance of four models with 882 training subjects, 219 validation subjects, and 1276 test subjects. Among the three classical machine learning algorithms, the bayesian ridge achieves the best performance. But the stacking model with

ensemble learning outperforms all of them, giving rise to the lowest MAE and MSE in both the validation and test set. More comparative results can be found in Supplementary Table S4. The correlation between chronological age and predicted age is presented in Fig. 2.

Table 1: Performance of four models.

Validation set			
Model	MAE	MSE	R <sup>2</sup>
Elastic Net	8.2327 ± 0.4608	103.7454 ± 10.9086	0.5670 ± 0.0486
Ridge	8.7749 ± 0.5662	127.4526 ± 17.7452	0.4691 ± 0.0665
Bayesian Ridge	7.8057 ± 0.4420	97.4546 ± 10.5659	0.5934 ± 0.0440
Stacking	7.7287 ± 0.5547	95.3625 ± 11.8727	0.6026 ± 0.0456
Test set			
Elastic Net	8.4156 ± 0.0582	110.2473 ± 1.2672	0.4839 ± 0.0059
Ridge	9.4921 ± 0.2447	143.8590 ± 6.8188	0.3265 ± 0.0319
Bayesian Ridge	8.3817 ± 0.0609	110.6582 ± 1.2202	0.4820 ± 0.0057
Stacking	8.3055 ± 0.0535	108.4852 ± 1.2633	0.4837 ± 0.0071

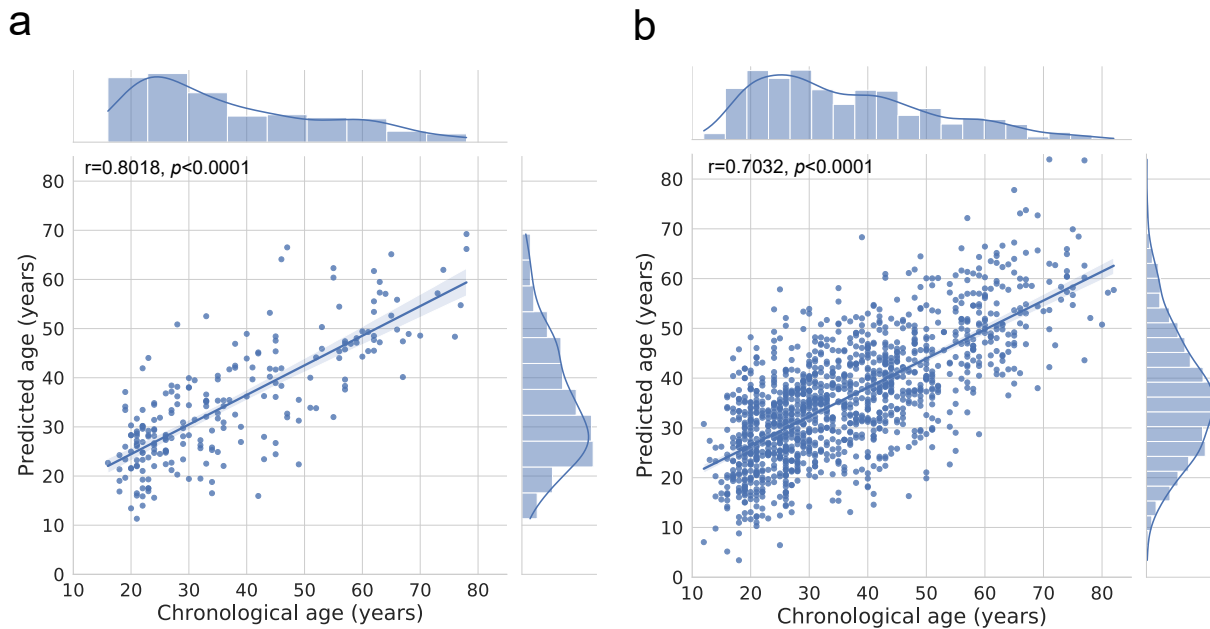


Fig. 2: Correlation between the chronological age (x-axis) and predicted age (y-axis) obtained by the stacking model on the validation set (a) and test set (b). Statistical values are obtained from Pearson correlations two-sided test. The lines represent the regression results and the shades correspond to the 95% confidence interval.

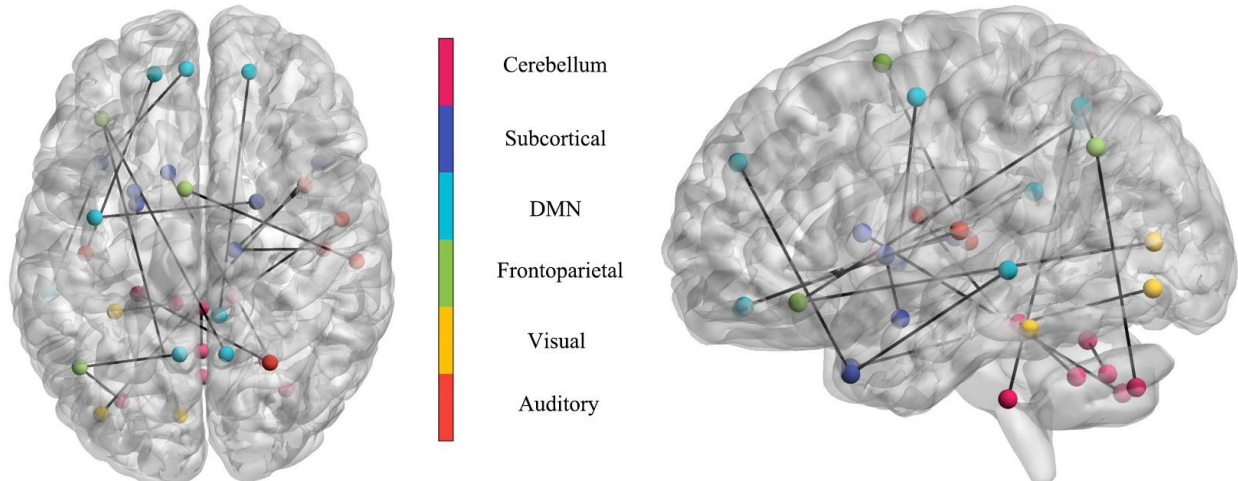


Fig. 3: The top 20 most important functional connectivity features obtained from the bayesian ridge model. These features consist of functional connectivity between the cerebellum superior and vermis8, medial superior frontal gyrus and middle temporal gyrus, amygdala and lenticular nucleus putamen, orbital inferior frontal gyrus and precuneus, angular gyrus and precuneus.

### 3.2. The relative feature importance for normal controls

We calculate the correlation between the functional connectivity features and the chronological age (Supplementary Fig. S6). Among all the total 6670 functional connectivity features, 3196 features show positive correlations with age (mean correlation =  $0.0645 \pm 0.0495$ , range( $6.1691e - 05, 0.3017$ )). 3474 features show negative correlations with age (mean correlation =  $-0.0691 \pm 0.0545$ , range( $-0.3334, 3.7818e - 05$ )). In particular, the most positive correlation is found for the precentral gyrus [52] - heschl gyrus [53]. The most negative correlation is found for the median cingulate and paracingulate gyri - inferior parietal gyrus, excluding supramarginal and angular gyri [54, 55]. In addition, we identify brain regions that the machine learning algorithm considers to be significant in the brain age estimation using the feature importance [56]. The feature importance values are normalized to give the top 20 functional connectivity features (Fig. 3). The main brain regions include the cerebellum [57] superior and vermis8, the medial superior frontal gyrus and middle temporal gyrus [58], the amygdala and lenticular nucleus putamen. These brain regions are associated with brain development and atrophy, which are consistent with previous studies. The detailed feature importance values are shown in Supplementary Fig. S7.

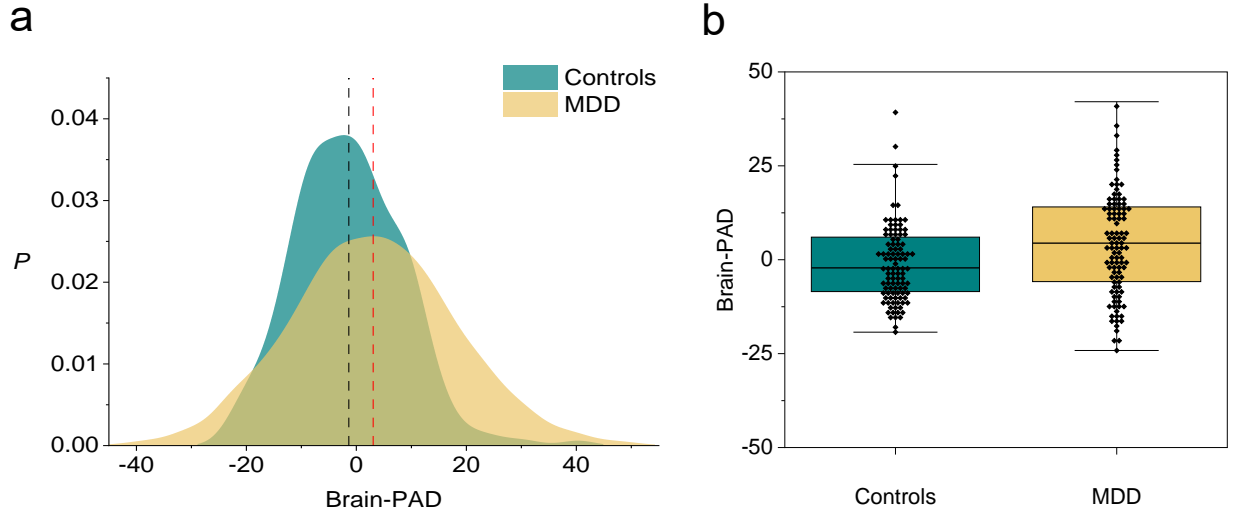


Fig. 4: Brain predicted age difference in controls and MDD patients. Group analysis shows that the corrected brain-PAD is significantly higher in MDD patients than in controls ( $p < 0.0001$ , Cohen’s  $d = 0.35$ , 95% CI : 1.86 – 3.91).

### 3.3. Accelerated functional brain aging in MDD

We compare the resulting brain-PAD scores of the MDD patients with the controls in the hold-out validation set to determine whether brain aging is accelerated in MDD patients. Overall, the brain-PAD score before age-bias correction is -1.3731 (SD 9.91) years in the control group and -0.0712 (SD 10.56) years in MDD patients. After applying an age-bias correction procedure, the brain-PAD is +4.43 years higher in MDD patients than in normal controls ( $p < 0.0001$ , Cohen’s  $d = 0.35$ , 95% CI : 1.86 – 3.91), which is shown in Fig. 4. Although different estimations are obtained through different models, results from the other three models all demonstrate a consistent pattern that MDD patients have a statistically significant higher brain-PAD scores compared to controls. In addition, GLM shows significant main effects for age ( $p < 0.001$ ), age<sup>2</sup> ( $p < 0.002$ ) and diagnosis ( $p < 0.0001$ ), but not for gender (Table 2).

### 3.4. Brain-PAD comparison for clinical characteristics

To explore the association between brain-PAD scores and clinical characteristics, we use the GLM to fit the brain-PAD of MDD patients with the following explanatory variables: sex, medication status, episode status, education years, and illness duration months (Table 3). The medication status ( $p = 0.023$ ) has a main effect on the brain-PAD scores of MDD

Table 2: Parameter estimates for all main effects and significant interactions in gender, diagnosis, age and age<sup>2</sup>.

	Coef	SE	$z$	$p$	[0.025	0.975]
Intercept	7.6400	2.570	2.972	0.003	2.602	12.678
Gender	-0.6052	0.771	-0.785	0.432	-2.116	0.905
Diagnosis	4.7237	1.045	4.519	0.000	2.675	6.772
Age	-0.4421	0.129	-3.433	0.001	-0.695	-0.190
Age <sup>2</sup>	0.0046	0.002	3.048	0.002	0.002	0.008

Table 3: Parameter estimates for all main effects and significant interactions in other clinical characteristics.

	Coef	SE	$z$	$p$	[0.025	0.975]
Intercept	1.8688	5.087	0.367	0.713	-8.102	11.839
Gender	-1.2863	1.255	-1.025	0.305	-3.746	1.173
Eposide	2.2518	1.532	1.470	0.141	-0.750	5.254
Medication	2.9454	1.291	2.282	0.023	0.415	5.475
Age	-0.0285	0.252	-0.113	0.910	-0.522	0.465
Age <sup>2</sup>	-0.0007	0.003	-0.219	0.827	-0.007	0.006
Education	-0.0022	0.156	-0.014	0.989	-0.307	0.303
Month	0.0060	0.012	0.511	0.609	-0.017	0.029

patients. We further apply a two-sample t-test to determine whether the brain-PAD mean value in antidepressant users and medication-free patients are significantly different from each other (Fig. 5). Brain-PAD is +2.09 years higher ( $p = 0.0499$ , Cohen’s  $d = 0.13$ ) in antidepressant users than in medication-free ones. Comparisons of other subgroups (sex, episode status) with controls can be found in Supplementary Table S5. While significant differences are observed in all MDD subgroups compared to normal controls, posthoc comparisons of brain-PAD in other clinical characteristics do not demonstrate any significant differences between MDD subgroups except for the medication status. For the two continuous-type clinical characteristics (education years and illness months), we divide the subgroups according to their medians (both are 12 in this study) for brain-PAD comparisons (Supplementary Table S6). Overall, MDD patients with fewer than 12 years of education have a 2.28 years higher brain-PAD than those with greater than or equal to 12 years of education

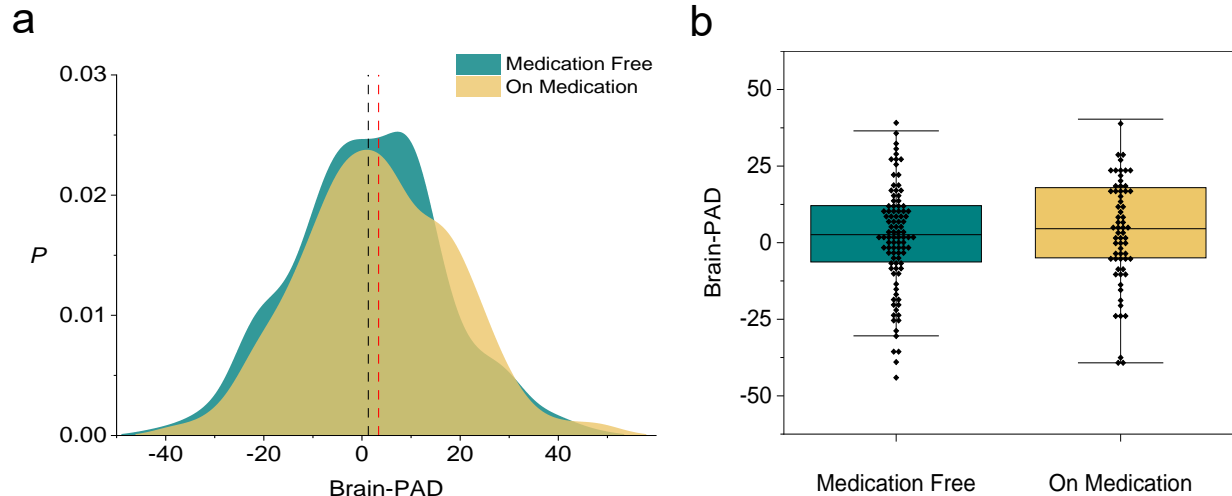


Fig. 5: Brain Predicted age difference in antidepressant users and medication-free patients. Group analysis shows that brain-PAD is higher in MDD patients who are taking medication (+3.38 years, 95% CI : 0.91 – 4.65) than in those medication-free ones (+1.29 years, 95% CI : -0.41 – 3.10). The difference passes the statistic significant threshold ( $p = 0.0499$ ).

( $p = 0.00679$ ). Brain-PAD of MDD patients with fewer than 12 months of illness is 1.69 years higher than that in patients with greater than or equal to 12 months of illness. We also calculate correlations between brain-PAD scores and illness months, education years, and HDRS scores separately. Only illness duration is found to be significantly correlated with brain-PAD scores (Spearman  $R = -0.067$ ,  $p < 0.05$ , Supplementary Fig. S8).

#### 4. DISCUSSION

Biological aging can be defined as a progressive process of decline involving multiple organ systems. While all individuals age chronologically at the same rate, the rate of their biological aging varies from one to the other [59]. Resting-state functional MRI is developed as a common approach to interrogate the myriad of functional systems in the brain without the constraints of any prior assumptions [60]. Machine learning algorithms based on functional connectivity and the availability of large-scale reliable samples allow us to develop generalized models to estimate the brain age of individual subjects [61]. Here, we make use of the Rest-Meta-MDD consortium from China to verify the accelerated brain aging in MDD patients, which is previously observed in Caucasian participants using structural MRI information. We apply four machine learning algorithms based on functional connectivity features to estimate the brain age of individuals with the entire adult lifespan (12-82 years).

We observe manifestly accelerated brain aging in 1276 MDD patients. Furthermore, we compare brain-PAD scores between MDD subgroups divided according to clinical characteristics such as medication status and episode status. We confirm that the conclusion drawn in this paper is not algorithm sensitive as results from different algorithms lead to the same conclusion.

Our study benefits from a reliable experimental design. The dataset contains 24 cohorts so the potential site effect is effectively avoided. Instead of using samples from some independent sites as the fixed validation set, we randomly select samples from all sites to constitute the training set and validation set. In this way, the generalizability of the model is improved and the model outcomes are evaluated more objectively [62, 63]. Moreover, we split the normal controls into a fixed training set and a hold-out validation set. We compare the brain-PAD scores of the controls in this hold-out validation set to the MDD patients in the test set. As the validation set is not involved in the development of the brain age prediction model, the risk of overfitting is effectively prevented [64]. The application of four different machine learning algorithms allows us to further validate the consistency of the patterns observed.

Although multiple studies are carried out on relatively small samples, conclusions drawn from larger samples tend to be more reliable. First, machine learning algorithms are sensitive to sample size [65–68]. The small size of samples brings a bigger prediction error and a higher risk of overfitting [69]. Moreover, larger samples tend to contain subjects with a wider age distribution. While a wide range of ages makes the estimation challenging, it effectively increases the generalizability of the conclusion [70]. In this study, we make use of the Rest-meta-MDD consortium, which is the largest rsfMRI database of MDD patients. To the best of our knowledge, only one study from ENIGMA uses more subjects than ours, which contains a total of 6989 subjects aged from 18 to 75 years old [30, 71]. But compared with ENIGMA, subjects in Rest-meta-MDD have a bigger life span, ranging from 12 to 82 years old (see the age distribution of the two datasets in Supplementary Fig. S4 and Fig. S5). The sufficiently large samples with a wider age span lead to similar conclusions drawn in ENIGMA.

Our results show a +4.43 years gap in terms of the brain-PAD between MDD patients and normal controls (with a Cohen’s  $d$  effect sizes size of 0.35) at the group level. Compared to previous studies on accelerated brain aging in MDD patients, such as the one by Koutsouleris

et al. [11] (+4.0 years, N = 104), Han et al. [30] (+1.16 years, N = 2675), Dunlop et al. [27] (+2.11 years, N = 112), Han et al. [24] (+0.586 years, N = 195), our results demonstrate a higher brain-PAD. We speculate that this may be related to the stigmatization of depression in traditional Chinese culture [72]. Some studies suggest that compared to Caucasians, Chinese tend to deny the existence of depression [73]. Consequently, the level of depression tends to be significantly elevated when MDD is diagnosed [74–76].

We find the significant main effects of age, age<sup>2</sup>, and diagnosis in our regression analysis. In particular, the main effect of medication status on brain-PAD is observed after the inclusion of other clinical characteristics, which is in line with the finding by Sacchet et al. [77]. The comparisons between subgroups of MDD patients show that antidepressant users have a statistically significant higher brain-PAD than medication-free patients (+2.09 years,  $p = 0.0499$ , Cohen’s  $d = 0.134483$ ). Explanations for this phenomenon are discussed by Han [30]. The antidepressant users are likely to have a more severe or chronic course of the disorder at the time of scanning. Therefore, the larger brain-PAD scores in antidepressant users may be confounded by clinical standards recommending antidepressant use mainly for severe or chronic MDD [78]. In other words, patients with milder symptoms tend not to take antidepressants [79]. To fully understand the adaptation of brain-PAD in response to pharmacotherapy, randomized controlled intervention studies are needed which require more information on the clinical use of antidepressants, such as the dosage and duration. It is also noteworthy that the  $p$ -value in the study by Han [30] is slightly above 0.05 whereas in our study it is slightly below the threshold of statistical significance. But it is still near the boundary of the threshold line. We honestly report the result, and we also admit that it is far early to draw any conclusion based on this statistic.

Similarly, consistent with the finding obtained by Han et al. [24] using structural brain MRI, we observe a higher brain-PAD in first-episode patients (+4.19 years, N = 538) than in recurrent patients (+2.56 years, N = 282). We believe the same explanation can be applied. First, as pointed out in previous studies and observed in our work, there is a negative correlation between the brain-PAD and illness duration (Spearman  $R = -0.067$ ,  $p < 0.05$ ). Furthermore, recurrent patients have a longer illness duration than first-episode patients. The median illness duration in recurrent patients (60 months) is 10 times greater than in first-episode patients (6 months) in our data. The corresponding median of brain-PAD score in recurrent patients (0.58 years) is 3.08 years smaller than in first-episode patients

(3.66 years). The combination of the two effects gives rise to a higher brain-PAD in first-episode patients than that in recurrent patients. It is implied that there may be a clinically unstable period in first-episode patients. As more treatment is given, patients may become more stable in brain functioning. Hence the brain-PAD decreases with the illness duration [24]. But such a hypothesis needs more clinical information to be further verified through longitudinal studies.

Our results extend the generalizability of accelerated brain aging in MDD patients using the rsfMRI feature of Chinese participants. But several limitations should be considered. Although a standardized preprocessing pipeline is employed at all sites before the aggregation group analysis, some subjects still show measurement bias and missing values in the scan. We address this problem by applying various standardization methods to the features. Although the prediction error is within the control, these operations may still bring impacts on the final results. Next, multiple brain atlas could be considered to obtain the functional connectivity features. Different functional connectivity will have an impact on the subsequent analysis. Furthermore, different features and models could also have a dramatic effect on the final results. Several studies report the great potential of the multimodal features [80–82] and deep learning algorithms [83–85] in neuroimaging research. More comparisons of neuroimaging features and models are needed in the future to produce more convincing conclusions. Besides, all participants in Rest-meta-MDD are Chinese, the generalizability of our model to other ethnic/racial and cultural backgrounds remained to be explored. Finally, aging is a continuous process, yet few current studies address longitudinal investigations of brain aging, including stage-by-stage analyses of MDD to explore trends in brain-PAD with age to understand the progressive effects of the aging process. More clinical features are still desired in the future to determine the clinical significance of measuring brain-PAD and whether it can be considered as a clinically essential biomarker.

## **ACKNOWLEDGMENTS**

This work is supported by Industry-University-Research Innovation Fund for Chinese Universities (No. 2021ALA03016), University Innovation Research Group of Chongqing (No. CXQT21005). We thank the REST-meta-MDD consortium for sharing the data.

- 
- [1] Vos, T., Flaxman, A. D., Naghavi, M. *et al.* Years lived with disability (ylds) for 1160 sequelae of 289 diseases and injuries 1990–2010: a systematic analysis for the global burden of disease study 2010. *The lancet* **380**, 2163–2196 (2012).
- [2] Dinsdale, N. K., Bluemke, E., Smith, S. M. *et al.* Learning patterns of the ageing brain in mri using deep convolutional networks. *Neuroimage* **224**, 117401 (2021).
- [3] Cole, J. H. & Franke, K. Predicting age using neuroimaging: innovative brain ageing biomarkers. *Trends in neurosciences* **40**, 681–690 (2017).
- [4] Harman, D. Aging: overview. *Annals of the New York Academy of Sciences* **928**, 1–21 (2001).
- [5] Isaev, N. K., Genrikhs, E. E., Oborina, M. V. *et al.* Accelerated aging and aging process in the brain. *Reviews in the Neurosciences* **29**, 233–240 (2018).
- [6] Dafflon, J., Pinaya, W. H., Turkheimer, F. *et al.* An automated machine learning approach to predict brain age from cortical anatomical measures. *Human brain mapping* **41**, 3555–3566 (2020).
- [7] Buckley, R. & Pascual-Leone, A. Age-related cognitive decline is indicative of neuropathology. *Annals of neurology* **87**, 813–815 (2020).
- [8] Kuo, C.-Y., Lee, P.-L., Hung, S.-C. *et al.* Large-scale structural covariance networks predict age in middle-to-late adulthood: A novel brain aging biomarker. *Cerebral Cortex* **30**, 5844–5862 (2020).
- [9] Mishra, S., Beheshti, I. & Khanna, P. A review of neuroimaging-driven brain age estimation for identification of brain disorders and health conditions. *IEEE Reviews in Biomedical Engineering* (2021).
- [10] Shahab, S., Mulsant, B. H., Levesque, M. L. *et al.* Brain structure, cognition, and brain age in schizophrenia, bipolar disorder, and healthy controls. *Neuropsychopharmacology* **44**, 898–906 (2019).
- [11] Koutsouleris, N., Davatzikos, C., Borgwardt, S. *et al.* Accelerated brain aging in schizophrenia and beyond: a neuroanatomical marker of psychiatric disorders. *Schizophrenia bulletin* **40**, 1140–1153 (2014).
- [12] Schnack, H. G., Van Haren, N. E., Nieuwenhuis, M. *et al.* Accelerated brain aging in schizophrenia: a longitudinal pattern recognition study. *American Journal of Psychiatry*

- 173**, 607–616 (2016).
- [13] Gonneaud, J., Baria, A. T., Pichet Binette, A. *et al.* Accelerated functional brain aging in pre-clinical familial alzheimer’s disease. *Nature communications* **12**, 1–17 (2021).
- [14] Moradi, E., Pepe, A., Gaser, C. *et al.* Machine learning framework for early mri-based alzheimer’s conversion prediction in mci subjects. *Neuroimage* **104**, 398–412 (2015).
- [15] Iturria-Medina, Y., Sotero, R. C., Toussaint, P. J. *et al.* Early role of vascular dysregulation on late-onset alzheimer’s disease based on multifactorial data-driven analysis. *Nature communications* **7**, 1–14 (2016).
- [16] Sone, D., Beheshti, I., Maikusa, N. *et al.* Neuroimaging-based brain-age prediction in diverse forms of epilepsy: a signature of psychosis and beyond. *Molecular psychiatry* **26**, 825–834 (2021).
- [17] Cole, J. H., Raffel, J., Friede, T. *et al.* Longitudinal assessment of multiple sclerosis with the brain-age paradigm. *Annals of neurology* **88**, 93–105 (2020).
- [18] Cole, J. H., Leech, R., Sharp, D. J. *et al.* Prediction of brain age suggests accelerated atrophy after traumatic brain injury. *Annals of neurology* **77**, 571–581 (2015).
- [19] Cole, J. H., Ritchie, S. J., Bastin, M. E. *et al.* Brain age predicts mortality. *Molecular psychiatry* **23**, 1385–1392 (2018).
- [20] Ferrari, A. J., Charlson, F. J., Norman, R. E. *et al.* Burden of depressive disorders by country, sex, age, and year: findings from the global burden of disease study 2010. *PLoS medicine* **10**, e1001547 (2013).
- [21] Verhoeven, J., Révész, D., Picard, M. *et al.* Depression, telomeres and mitochondrial dna: between-and within-person associations from a 10-year longitudinal study. *Molecular psychiatry* **23**, 850–857 (2018).
- [22] Verhoeven, J. E., Révész, D., Epel, E. S. *et al.* Major depressive disorder and accelerated cellular aging: results from a large psychiatric cohort study. *Molecular psychiatry* **19**, 895–901 (2014).
- [23] John, A., Patel, U., Rusted, J. *et al.* Affective problems and decline in cognitive state in older adults: a systematic review and meta-analysis. *Psychological medicine* **49**, 353–365 (2019).
- [24] Han, S., Chen, Y., Zheng, R. *et al.* The stage-specifically accelerated brain aging in never-treated first-episode patients with depression. *Human Brain Mapping* (2021).

- [25] Christman, S., Bermudez, C., Hao, L. *et al.* Accelerated brain aging predicts impaired cognitive performance and greater disability in geriatric but not midlife adult depression. *Translational Psychiatry* **10**, 1–11 (2020).
- [26] Kaufmann, T., van der Meer, D., Doan, N. T. *et al.* Common brain disorders are associated with heritable patterns of apparent aging of the brain. *Nature neuroscience* **22**, 1617–1623 (2019).
- [27] Dunlop, K., Victoria, L. W., Downar, J. *et al.* Accelerated brain aging predicts impulsivity and symptom severity in depression. *Neuropsychopharmacology* **46**, 911–919 (2021).
- [28] Drobinin, V., Van Gestel, H., Helmick, C. A. *et al.* The developmental brain age is associated with adversity, depression, and functional outcomes among adolescents. *Biological Psychiatry: Cognitive Neuroscience and Neuroimaging* (2021).
- [29] Besteher, B., Gaser, C. & Nenadić, I. Machine-learning based brain age estimation in major depression showing no evidence of accelerated aging. *Psychiatry Research: Neuroimaging* **290**, 1–4 (2019).
- [30] Han, L. K., Dinga, R., Hahn, T. *et al.* Brain aging in major depressive disorder: results from the enigma major depressive disorder working group. *Molecular psychiatry* 1–16 (2020).
- [31] Vergun, S., Deshpande, A., Meier, T. B. *et al.* Characterizing functional connectivity differences in aging adults using machine learning on resting state fmri data. *Frontiers in computational neuroscience* **7**, 38 (2013).
- [32] Yan, C.-G., Chen, X., Li, L. *et al.* Reduced default mode network functional connectivity in patients with recurrent major depressive disorder. *Proceedings of the National Academy of Sciences* **116**, 9078–9083 (2019).
- [33] Yang, H., Chen, X., Chen, Z.-B. *et al.* Disrupted intrinsic functional brain topology in patients with major depressive disorder. *Molecular psychiatry* 1–9 (2021).
- [34] Liem, F., Varoquaux, G., Kynast, J. *et al.* Predicting brain-age from multimodal imaging data captures cognitive impairment. *Neuroimage* **148**, 179–188 (2017).
- [35] Zhai, J. & Li, K. Predicting brain age based on spatial and temporal features of human brain functional networks. *Frontiers in human neuroscience* **13**, 62 (2019).
- [36] Li, H., Satterthwaite, T. D. & Fan, Y. Brain age prediction based on resting-state functional connectivity patterns using convolutional neural networks. In *2018 IEEE 15th International Symposium on Biomedical Imaging (ISBI 2018)*, 101–104 (IEEE, 2018).

- [37] Yan, C. & Zang, Y. Dparsf: a matlab toolbox for” pipeline” data analysis of resting-state fmri. *Frontiers in systems neuroscience* **4**, 13 (2010).
- [38] Ball, G., Kelly, C. E., Beare, R. *et al.* Individual variation underlying brain age estimates in typical development. *NeuroImage* **235**, 118036 (2021).
- [39] Khundrakpam, B. S., Tohka, J., Evans, A. C. *et al.* Prediction of brain maturity based on cortical thickness at different spatial resolutions. *Neuroimage* **111**, 350–359 (2015).
- [40] Xu, Y., Li, X., Yang, Y. *et al.* Human age prediction based on dna methylation of non-blood tissues. *Computer methods and programs in biomedicine* **171**, 11–18 (2019).
- [41] Niu, X., Zhang, F., Kounios, J. *et al.* Improved prediction of brain age using multimodal neuroimaging data. *Human brain mapping* **41**, 1626–1643 (2020).
- [42] Chung, Y., Addington, J., Bearden, C. E. *et al.* Use of machine learning to determine deviance in neuroanatomical maturity associated with future psychosis in youths at clinically high risk. *JAMA psychiatry* **75**, 960–968 (2018).
- [43] Couvy-Duchesne, B., Faouzi, J., Martin, B. *et al.* Ensemble learning of convolutional neural network, support vector machine, and best linear unbiased predictor for brain age prediction: Aramis contribution to the predictive analytics competition 2019 challenge. *Frontiers in psychiatry* **11** (2020).
- [44] Da Costa, P. F., Dafflon, J. & Pinaya, W. H. Brain-age prediction using shallow machine learning: predictive analytics competition 2019. *Frontiers in psychiatry* **11** (2020).
- [45] Levman, J., Jennings, M., Kabaria, P. *et al.* Hold-out validation for the assessment of stability and reliability of multivariable regression demonstrated with magnetic resonance imaging of patients with schizophrenia. *International Journal of Developmental Neuroscience* **81**, 655–662 (2021).
- [46] Smith, S. M., Vidaurre, D., Alfaro-Almagro, F. *et al.* Estimation of brain age delta from brain imaging. *Neuroimage* **200**, 528–539 (2019).
- [47] Le, T. T., Kuplicki, R. T., McKinney, B. A. *et al.* A nonlinear simulation framework supports adjusting for age when analyzing brainage. *Frontiers in aging neuroscience* **10**, 317 (2018).
- [48] Liang, H., Zhang, F. & Niu, X. Investigating systematic bias in brain age estimation with application to post-traumatic stress disorders. Tech. Rep., Wiley Online Library (2019).
- [49] Cole, J. H. Multimodality neuroimaging brain-age in uk biobank: relationship to biomedical, lifestyle, and cognitive factors. *Neurobiology of aging* **92**, 34–42 (2020).

- [50] Aycheh, H. M., Seong, J.-K., Shin, J.-H. *et al.* Biological brain age prediction using cortical thickness data: a large scale cohort study. *Frontiers in aging neuroscience* **10**, 252 (2018).
- [51] Peng, H., Gong, W., Beckmann, C. F. *et al.* Accurate brain age prediction with lightweight deep neural networks. *Medical image analysis* **68**, 101871 (2021).
- [52] Kovalev, V. A., Kruggel, F. & von Cramon, D. Y. Gender and age effects in structural brain asymmetry as measured by mri texture analysis. *NeuroImage* **19**, 895–905 (2003).
- [53] Amoroso, N., La Rocca, M., Bellantuono, L. *et al.* Deep learning and multiplex networks for accurate modeling of brain age. *Frontiers in aging neuroscience* **11**, 115 (2019).
- [54] MacDonald, S. W., Nyberg, L., Sandblom, J. *et al.* Increased response-time variability is associated with reduced inferior parietal activation during episodic recognition in aging. *Journal of Cognitive Neuroscience* **20**, 779–786 (2008).
- [55] Rivera, S. M., Reiss, A., Eckert, M. A. *et al.* Developmental changes in mental arithmetic: evidence for increased functional specialization in the left inferior parietal cortex. *Cerebral cortex* **15**, 1779–1790 (2005).
- [56] Hellyer, P. J., Leech, R., Ham, T. E. *et al.* Individual prediction of white matter injury following traumatic brain injury. *Annals of neurology* **73**, 489–499 (2013).
- [57] Tiemeier, H., Lenroot, R. K., Greenstein, D. K. *et al.* Cerebellum development during childhood and adolescence: a longitudinal morphometric mri study. *Neuroimage* **49**, 63–70 (2010).
- [58] Tomoda, A., Kinoshita, S., Korenaga, Y. *et al.* Pseudohypacusis in childhood and adolescence is associated with increased gray matter volume in the medial frontal gyrus and superior temporal gyrus. *Cortex* **48**, 492–503 (2012).
- [59] Elliott, M. L., Caspi, A., Houts, R. M. *et al.* Disparities in the pace of biological aging among midlife adults of the same chronological age have implications for future frailty risk and policy. *Nature aging* **1**, 295–308 (2021).
- [60] Biswal, B. B., Mennes, M., Zuo, X.-N. *et al.* Toward discovery science of human brain function. *Proceedings of the National Academy of Sciences* **107**, 4734–4739 (2010).
- [61] Franke, K. & Gaser, C. Ten years of brainage as a neuroimaging biomarker of brain aging: what insights have we gained? *Frontiers in neurology* **10**, 789 (2019).
- [62] Orrù, G., Monaro, M., Conversano, C. *et al.* Machine learning in psychometrics and psychological research. *Frontiers in psychology* **10**, 2970 (2020).

- [63] Cai, X.-L., Xie, D.-J., Madsen, K. H. *et al.* Generalizability of machine learning for classification of schizophrenia based on resting-state functional mri data. *Human brain mapping* **41**, 172–184 (2020).
- [64] Shim, M., Lee, S.-H. & Hwang, H.-J. Inflated prediction accuracy of neuropsychiatric biomarkers caused by data leakage in feature selection. *Scientific Reports* **11**, 1–7 (2021).
- [65] Arbabshirani, M. R., Plis, S., Sui, J. *et al.* Single subject prediction of brain disorders in neuroimaging: Promises and pitfalls. *Neuroimage* **145**, 137–165 (2017).
- [66] Gianfrancesco, M. A., Tamang, S., Yazdany, J. *et al.* Potential biases in machine learning algorithms using electronic health record data. *JAMA internal medicine* **178**, 1544–1547 (2018).
- [67] Varoquaux, G. Cross-validation failure: small sample sizes lead to large error bars. *Neuroimage* **180**, 68–77 (2018).
- [68] Vabalas, A., Gowen, E., Poliakoff, E. *et al.* Machine learning algorithm validation with a limited sample size. *PloS one* **14**, e0224365 (2019).
- [69] Marek, S., Tervo-Clemmens, B., Calabro, F. J. *et al.* Reproducible brain-wide association studies require thousands of individuals. *Nature* 1–7 (2022).
- [70] Cole, J. H., Franke, K. & Cherbuin, N. Quantification of the biological age of the brain using neuroimaging. In *Biomarkers of human aging*, 293–328 (Springer, 2019).
- [71] Schmaal, L., Pozzi, E., Ho, T. C. *et al.* Enigma mdd: seven years of global neuroimaging studies of major depression through worldwide data sharing. *Translational psychiatry* **10**, 1–19 (2020).
- [72] Georg Hsu, L., Wan, Y. M., Chang, H. *et al.* Stigma of depression is more severe in chinese americans than caucasian americans. *Psychiatry: Interpersonal and Biological Processes* **71**, 210–218 (2008).
- [73] Parker, G., Gladstone, G. & Chee, K. T. Depression in the planet’s largest ethnic group: the chinese. *American Journal of Psychiatry* **158**, 857–864 (2001).
- [74] Young, C. B., Fang, D. Z. & Zisook, S. Depression in asian–american and caucasian undergraduate students. *Journal of affective disorders* **125**, 379–382 (2010).
- [75] Ai, A. L., Nicdao, E. G., Appel, H. B. *et al.* Ethnic identity and major depression in asian american subgroups nationwide: Differential findings in relation to subcultural contexts. *Journal of Clinical Psychology* **71**, 1225–1244 (2015).

- [76] Krieg, A., Xu, Y. & Cicero, D. C. Comparing social anxiety between asian americans and european americans: An examination of measurement invariance. *Assessment* **25**, 564–577 (2018).
- [77] Sacchet, M. D., Camacho, M. C., Livermore, E. E. *et al.* Accelerated aging of the putamen in patients with major depressive disorder. *Journal of psychiatry & neuroscience: JPN* **42**, 164 (2017).
- [78] Schmaal, L., Hibar, D., Sämann, P. G. *et al.* Cortical abnormalities in adults and adolescents with major depression based on brain scans from 20 cohorts worldwide in the enigma major depressive disorder working group. *Molecular psychiatry* **22**, 900–909 (2017).
- [79] Schmaal, L., Veltman, D. J., van Erp, T. G. *et al.* Subcortical brain alterations in major depressive disorder: findings from the enigma major depressive disorder working group. *Molecular psychiatry* **21**, 806–812 (2016).
- [80] Cherubini, A., Caligiuri, M. E., Péran, P. *et al.* Importance of multimodal mri in characterizing brain tissue and its potential application for individual age prediction. *IEEE journal of biomedical and health informatics* **20**, 1232–1239 (2016).
- [81] De Lange, A.-M. G., Anatürk, M., Suri, S. *et al.* Multimodal brain-age prediction and cardiovascular risk: The whitehall ii mri sub-study. *NeuroImage* **222**, 117292 (2020).
- [82] Rokicki, J., Wolfers, T., Nordhøy, W. *et al.* Multimodal imaging improves brain age prediction and reveals distinct abnormalities in patients with psychiatric and neurological disorders. *Human brain mapping* **42**, 1714–1726 (2021).
- [83] Jónsson, B. A., Bjornsdottir, G., Thorgeirsson, T. *et al.* Brain age prediction using deep learning uncovers associated sequence variants. *Nature communications* **10**, 1–10 (2019).
- [84] Schulz, M.-A., Yeo, B. T., Vogelstein, J. T. *et al.* Different scaling of linear models and deep learning in ukbiobank brain images versus machine-learning datasets. *Nature communications* **11**, 1–15 (2020).
- [85] Abrol, A., Fu, Z., Salman, M. *et al.* Deep learning encodes robust discriminative neuroimaging representations to outperform standard machine learning. *Nature communications* **12**, 1–17 (2021).
- [86] Shamaei, E. & Kaedi, M. Suspended sediment concentration estimation by stacking the genetic programming and neuro-fuzzy predictions. *Applied Soft Computing* **45**, 187–196 (2016).

## SUPPLEMENTARY INFORMATION

### S1. Data acquisition

The REST-meta-MDD consortium contains a total of 25 neural cohorts from incoming groups in China. Site 4 (including 24 MDD patients and 24 controls) is excluded in that it is a duplicate of site 14 (detected during the preparation of REST-meta-MDD data for open sharing). We construct a functional connectivity network for each subject based on the AAL atlas using time series data from subjects at the remaining 24 sites. The specific information for each site is shown in Table S1 and Tabel S2. We take the step of adjusting the characteristics of all subjects by various normalization methods. Although these operations may have a slight effect on the final results, we consider these errors to be within reasonable control.

### S2. Data preprocessing and quality control

The initial 10 functional images are discarded with the slice acquisition timing discrepancies and the head motion is performed. Linear trends, friston 24 head motion parameters, the white matter signal, and the cerebrospinal fluid signal are regressed out from the functional signal as nuisance covariates. Our quality control is more relaxed compared to previous studies. We only remove duplicate samples from site 4 and three samples with abnormal age, resulting in 1276 MDD patients and 1101 controls. Various types of subjects are removed in Yan et al. [32] and Yang et al. [33], such as subjects from small sample sites, subjects younger than 18 or older than 65, subjects with vacancies in clinical characteristics, etc. We believe that the age distribution of the training set needs to be made as wide as possible for the model to have better generalizability. At the same time, the proposed algorithm predicts the brain age of subjects based on rsFC features, and the vacancies in clinical features do not affect the algorithm to predict the brain age of subjects based on their rsFC features.

### S3. Stacking model

Stacking model is an ensemble learning approach that combines different prediction models in a single model, working at levels or layers. This approach aims to minimize the errors of

generalization by reducing the bias of its generalizers. Considering a stacking approach using two levels (level-0 and level-1) in Fig. S1. In level-0, diverse base models are trained, and the prediction of the response variable for each one is performed subsequently. These forecasts are used as a new input feature for the level-1 model, which is also called meta-model [86]. At the same time, the base classifiers need to predict the test set, and the predictions are averaged as a new test set for the meta classifier to predict the desired result.

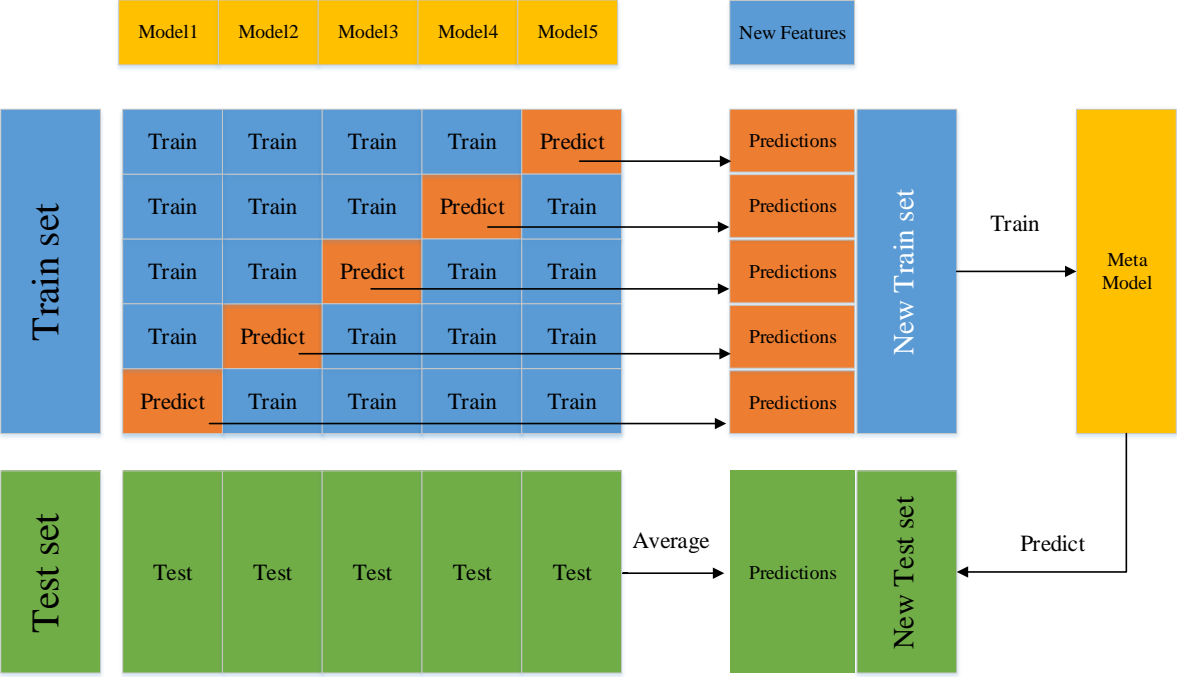


Fig. S1: Schematic diagram of two levels stacking.

#### S4. Correcting the age dependence of brain-PAD

As shown in Fig. S2a and Fig. S3a, following many existing studies, we observe a significant correlation between brain-PAD and chronological age. It means that the predicted age tends to be biased towards the mean age of the cohort, implying that younger subjects will be predicted to be older and vice versa. To correct for the presence of regression dilution bias in age prediction, we train a linear regression model to fit the predicted age on the validation set with age labels set aside. Then the slope and intercept of this model are used to correct for the predicted age from the test set. The corrected predicted age and the correlation between corrected brain-PAD and chronological age are shown in Fig. S2b and Fig. S3b. Following Peng et al. [51], we define  $y$  to be chronological age and  $x$  to be the predicted age, and we fit a linear regression (Equation 1) to the hold-out validation set (with labels). The corrected predicted age is estimated by Equation 2.

$$x = ay + b \tag{1}$$

$$\hat{x} = \frac{x - b}{a} \tag{2}$$

This method requires (at the point of estimating  $a$  and  $b$  from  $x$  and  $y$ ) that the chronological ages are known. For the label-missing (final evaluation) test set, we assume that  $a$  and  $b$  are generalizable, and use the coefficients previously fit in the hold-out validation set to estimate the brain age.

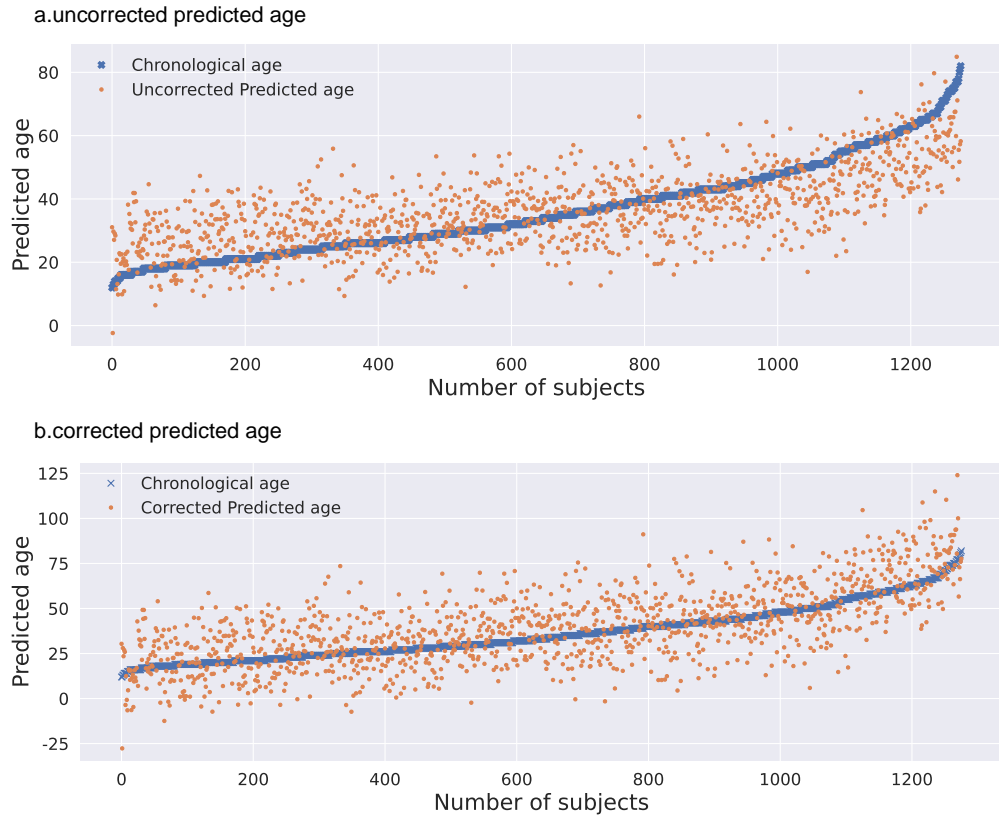


Fig. S2: Comparison of predicted age before and after correction.

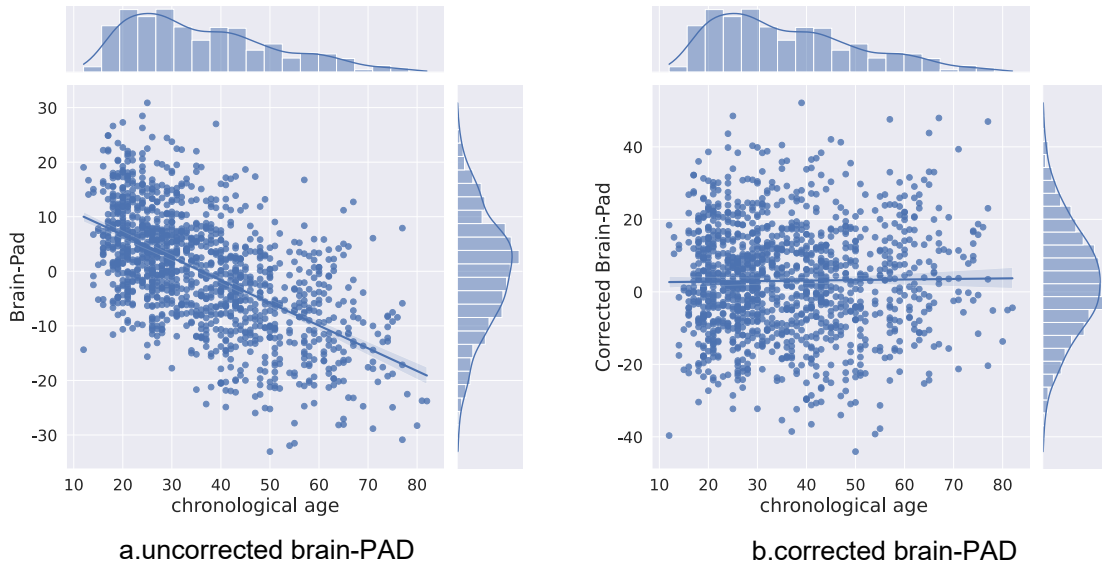


Fig. S3: Correlation between bran-PAD and chronological age before and after correction.

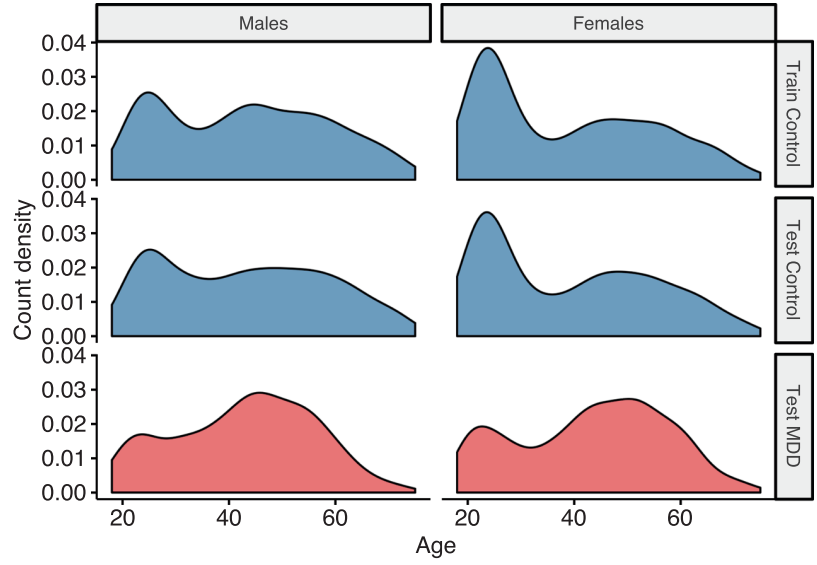


Fig. S4: Age distribution in ENIGMA. The ENIGMA MDD Working Group contains 6989 participants (18-75 years old).

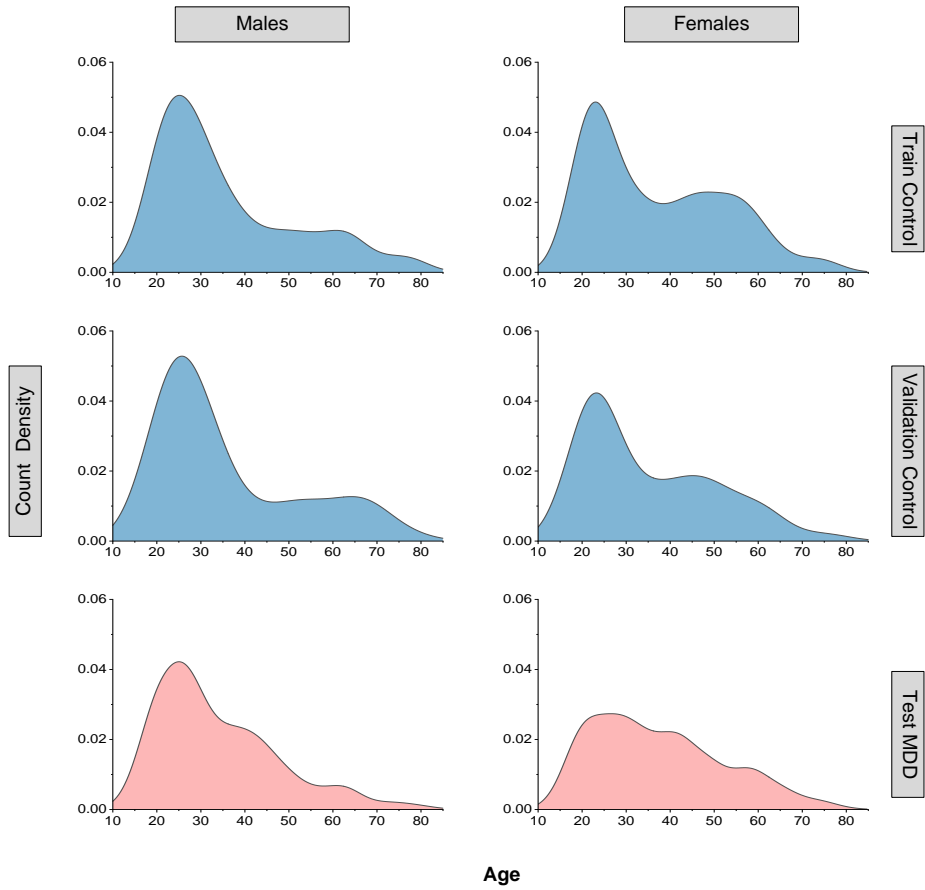


Fig. S5: Age distribution in Rest-meta-MDD. The Rest-meta-MDD contains 2377 participants (12-82 years old).

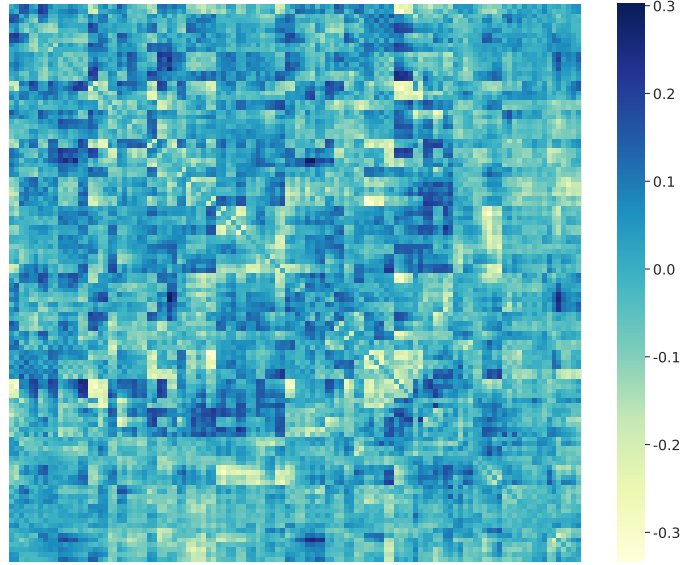


Fig. S6: Correlation between the functional connectivity features and the chronological age. Among all the total 6670 functional connectivity features, 3196 features show positive correlations with age mean correlation =  $0.0645 \pm 0.0495$ , range( $6.1691e - 05, 0.3017$ ). 3474 features show negative correlations with age mean correlation =  $-0.0691 \pm 0.0545$  with range( $-0.3334, 3.7818e - 05$ ).

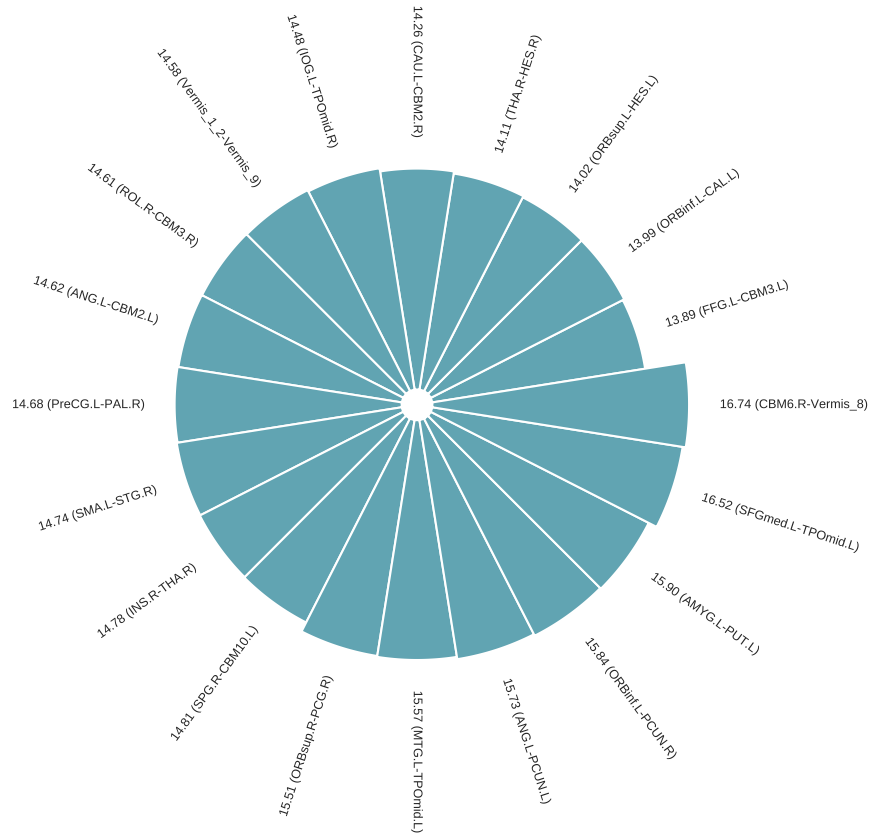


Fig. S7: The top 20 feature importance value. The values of all feature importance are normalized by a factor of 100. The maximum value is 16.736843 for the correlation between cerebellum superiorR and vermis8.

Table S1: Samples of selected sites.

Serial number	Research groups	MDD patients (n)	NCs (n)
1	National Clinical Research Center for Mental Disorders, Peking University	74	74
2	The Affiliated Guangji Hospital of Soochow University	30	30
3	The Second Xiangya Hospital of Central South University	27	37
5	Department of Psychiatry, Shanghai Jiao Tong University School of Medicine	13	11
6	Department of Psychiatry, Shanghai Jiao Tong University School of Medicine	15	15
7	Sir Run Run Shaw Hospital, Zhejiang University School of Medicine	38	49
8	Department of Psychiatry, First Affiliated Hospital, China Medical University	75	75
9	The First Affiliated Hospital of Jinan University	50	50
10	First Hospital of Shanxi Medical University	50	33
11	Department of Psychiatry, The First Affiliated Hospital of Chongqing Medical University	32	29
12	Department of Psychiatry, The First Affiliated Hospital of Chongqing Medical University	32	6
13	The First Affiliated Hospital of Xi'an Jiaotong University, Xian Central Hospital	25	17
14	The Second Xiangya Hospital of Central South University	64	32
15	Zhongda Hospital, School of Medicine, Southeast University	50	50
16	Huaxi MR Research Center, West China Hospital of Sichuan University	31	31
17	Department of Psychiatry, The First Affiliated Hospital of Chongqing Medical University	47	44
18	The First Affiliated Hospital, College of Medicine, Zhejiang University	21	20
19	Anhui Medical University	51	36
20	Faculty of Psychology, Southwest University	282	251
21	Beijing Anding Hospital, Capital Medical University	86	70
22	The Institute of Mental Health, Second Xiangya Hospital of Central South University	30	20
23	Mental Health Center, West China Hospital, Sichuan University	32	30
24	First Affiliated Hospital of Kunming Medical University	32	31
25	Department of Neurology, Affiliated ZhongDa Hospital of Southeast University	89	63

Table S2: Data acquisition parameters of selected sites.

Serial number	Scanner	Coil	TR (ms)	TE (ms)	Flip angle	Thickness/gap	Slice number	Timepoints	Voxel size	FOV
1	Siemens Tim Trio 3T	32	2000	30	90	4.0 mm/0.8 mm	30	210	3.28*3.28*4.80	210*210
2	Philips Achieva 3T	8	2000	30	90	4.0 mm/0 mm	37	200	1.67*1.67*4.00	240*240
3	Siemens 1.5 T	16	2000	40	90	5.0mm/1.25mm	26	150	3.75*3.75*6.25	240*240
5	GE Signa 3T	32	3000	30	90	5.0mm/0 mm	22	100	3.75*3.75*5.00	240*240
6	Siemens Tim Trio 3T	32	2000	30	70	4mm/0mm	33	180	3.59*3.59*4.00	230*230
7	GE discovery MR750	8	2000	30	90	3.2 mm/0 mm	37	184	2.29*2.29*3.20	220*220
8	GE Signa 3T	8	2000	30	90	3.0 mm/0 mm	35	200	3.75*3.75*3.00	240*240
9	GE Discovery MR750 3.0T	8	2000	25	90	3.0 mm/1.0 mm	35	200	3.75*3.75*4.00	240*240
10	Siemens Tim Trio 3T	32	2000	30	90	3.0 mm/1.52 mm	32	212	3.75*3.75*4.52	240*240
11	GE Signa 3T	8	2000	30	90	5 mm	33	200	3.75*3.75*5.00	240*240
12	GE Signa 3T	8	2000	30	90	5 mm	33	240	3.75*3.75*4.00	240*240
13	GE Excite 1.5T	16	2500	35	90	4 mm/0 mm	36	150	4.00*4.00*4.00	256*256
14	Siemens Tim Trio 3T	32	2500	25	90	3.5 mm/0 mm	39	200	3.75*3.75*3.50	240*240
15	Siemens Verio 3.0T MRI	12	2000	25	90	4 mm/0 mm	36	240	3.75*3.75*4.00	240*240
16	GE Signa 3T	8	2000	30	90	5mm/0mm	30	200	3.75*3.75*5.00	240*240
17	GE Signa 3T	8	2000	40	90	4.0 mm/0 mm	33	240	3.75*3.75*4.00	240*240
18	Philips Achieva 3.0 T scanner	8	2000	35	90	5.0/1.0 mm	24	200	1.67*1.67*6.00	240*240
19	GE Signa 3T	8	2000	22.5	30	4.0 mm/0.6 mm	33	240	3.44*3.44*4.60	220*220
20	Siemens Tim Trio 3T	12	2000	30	90	3.0 mm/1.0 mm	32	242	3.44*3.44*4.00	220*220
21	Siemens Tim Trio 3T	32	2000	30	90	3.5 mm/0.7 mm	33	240	3.12*3.12*4.20	200*200
22	Philips Gyroscaan Achieva 3.0T	32	2000	30	90	4.0 mm/0 mm	36	250	1.67*1.67*4.00	240*240
23	Philips Achieva 3.0T TX	8	2000	30	90	4.0 mm/0 mm	38	240	3.75*3.75*4.00	240*240
24	GE Signa 1.5T	8	2000	40	90	5/1mm	24	160	3.75*3.75*6.00	240*240
25	Siemens Verio 3T	12	2000	25	90	4.0mm/0 mm	36	240	3.75*3.75*4.00	240*240

Table S3: Comparison of brain-PAD in different models.

Model	MDD-NC(Mean-PAD)	<i>P</i> value	Cohen's <i>d</i>
SVM-linear	5.215	4.09e-09	0.367
EN	3.282	5.88e-05	0.255
Ridge	5.186	5.22e-09	0.364
BR	4.532	3.55e-08	0.348

Table S4: Performance of different models.

Validation set			
Model	MAE	MSE	R <sup>2</sup>
SVM-linear	8.9308 ± 0.6309	132.4733 ± 20.3135	0.4482 ± 0.0771
SVM-RBF	11.6761 ± 0.8564	231.1530 ± 30.6658	0.04127 ± 0.0647
RandomForest	15.1180 ± 1.3921	433.7388 ± 57.8672	-0.8006 ± 0.1541
XGBoost	23.3025 ± 1.8482	776.5373 ± 110.7799	-2.2516 ± 0.5404
Test set			
SVM-linear	9.6537 ± 0.3379	148.42189 ± 9.4821	0.3051 ± 0.0443
SVM-RBF	11.0753 ± 0.0464	205.1567 ± 3.4306	0.0395 ± 0.0160
RandomForest	15.4476 ± 0.1794	408.0862 ± 8.6558	-0.9104 ± 0.0405
XGBoost	34.2420 ± 0.1923	1590.5002 ± 22.9607	-6.4457 ± 0.1074

Table S5: Comparison of brain-PAD between different clinical characteristics.

MDD vs NC	Number Brain-PAD	<i>P</i> value	SD	Cohen's <i>d</i>	95% CI	
MDD	1276	4.43	3.49e-08	15	0.35	1.86-3.91
First-episode MDD	538	4.19	7.80e-06	14.99	0.33	1.63-4.83
Recurrent episode	282	2.56	2.10e-02	14.85	0.2	-4.51
antidepressant users	408	4.75	3.99e-06	15.62	0.36	0.91-4.65
Medication free	447	2.66	7.16e-03	15.41	0.21	-3.43
Male	463	5.07	1.85e-07	14.89	0.4	1.60-4.83
Female	813	4.06	2.30e-06	15.06	0.32	1.37-3.90

Table S6: Comparison of brain-PAD in education years and illness duration months.

MDD subgroup	Number	Brain-PAD
Education <12	634	4.2
Education ≥12	642	1.92
Duration <6	329	4.05
Duration <12	461	3.7
6 ≤ Duration <12	132	2.83
12 ≤ Duration <24	130	2.48
Duration ≥12	524	2.01
Duration ≥24	394	1.86

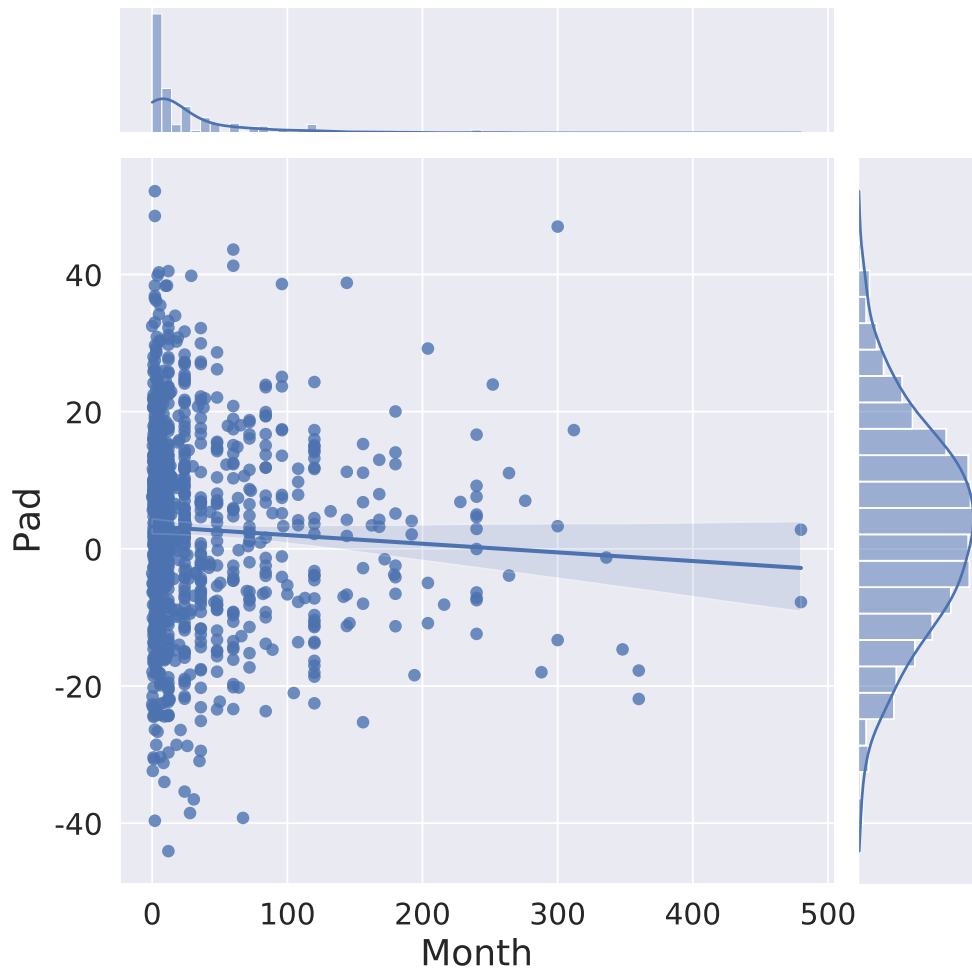


Fig. S8: The correlation between brain-PAD scores and illness duration months in patients with depression. There is a negative correlation between the brain-PAD and illness duration (Spearman  $R = -0.067$ ,  $p = 0.03$ ).